Radiation Tolerance of Cold 65 nm Process Pixel Readout Electronics to MeV Gammas

Zachary Franklin, Department of Physics

April 17, 2024

Thesis Advisor: Professor Stephen Wagner, Physics
Honors Council Representative: Professor John Cumalat, Physics
Outside Reader: Professor Nikolaus Correll, Computer Science

Abstract

Radiation can affect electronics in a number of ways and alter their behavior. The inner tracker of the CMS experiment has sensors and readout chips near the beam line. With the High-Luminosity Large Hydron collider, the dose rate for these electronics will increase, and so will the risk of failure. In order to ensure these electronics can last years near the beam, we must test them with ionizing particles. Experiments have been conducted using X-ray beams, but our irradiation looked for effects of approximately 1 MeV gamma radiation on the readout chips. As the readout chips will be within a meter of the beamline, they will likely see particles of higher energy than X-rays, and it is essential to research how these particles affect the electronics over the course of irradiation up to 1 GRad. We saw some stark differences between the X-ray groups results and our own results. The voltages on the card seem to change less for the gamma-ray irradiation than for the X-ray irradiation, seeming like our chip is acquiring less damage. However, there was more damage to the connection between the aluminum wire bonds and the electroless nickel immersion gold wire bond pads on the SCC. These results show that the chip may be damaged less by gamma rays than by X-rays, except for the wire bonds, for which our irradiation seems to have caused a reaction that damages the wire bonds.

Contents

Tables

Figures

Background Information

CMS Inner Tracker

The Compact Muon Solenoid (CMS) Experiment is a particle detector at the Large Hadron Collider in CERN Switzerland. The LHC collides particles at four different positions along its ring, and the CMS experiment sits on one of these points. It does not have a specific purpose and is looking for a myriad of exciting physics, from studying the Standard Model to trying to detect dark matter. The CMS experiment helped discover the Higgs Boson in 2012 alongside the ATLAS Experiment. The detector has multiple different features for collecting data.

The detector has many layers to it, each with different responsibilities. One layer is the solenoid, from which the CMS detector is named. This solenoid is one of the most powerful superconducting solenoids ever made and produces a 3.8 Tesla Magnetic field parallel to the beamline. This magnetic field bends the particles produced by the colliding beams at the beam interaction point. The bending of these particles allows us to tell the particles' charge and momentum. However, these calculations require us to measure the particle's path; to do this, we need information about the particle's position.

The innermost layer of the detector is the Inner Tracker positioned within a quarter of a meter from the beam line.[4] This layer consists of 4 cylindrical layers of silicon pixel detectors and discs of sensors on either side of the interaction point. These layers have roughly 124 million pixels, which allows us to detect particles very accurately. For a 50μm by 50μm pixel, it is part of a sensor that is about 16.8mm by 16.8mm and contains about 153600 of these individual pixels.[6, p. 7] This is just an example. Other pixels come in different dimensions and are better at measuring particle positions along different dimensions.

Silicon Pixel sensors

Silicon pixels are a very important part of the CMS experiment. They allow us to record the position of particles very close to the beamline where track densities are

highest. Calculating their charge and momentum from the curvature of their paths can be done once we have these positions. Silicon pixel sensors are a magnificent feat of science. Silicon pixels use the special properties of silicon to collect charge and produce a signal from the ionizing particle. This signal, in turn, allows us to analyze this signal and determine whether an ionizing particle was present.

Silicon pixels utilize the semiconducting properties of silicon. A band gap energy is the energy required for electrons and holes (empty electron positions in the valence band) to transition from the valence band to the conduction band. Semiconductors have a small non-zero band gap energy; for plain silicon, this energy is 1.12 eV. To utilize these semiconductor properties, we must dope the silicon with four valence electron elements like phosphorus to make an n-type material or three valence electron elements like boron to make a p-type material. N-type materials have a higher concentration of electrons, and p-type materials have higher concentrations of holes. These new materials have properties where an electric field is generated between them if they are in contact. For the silicon to reach equilibrium, electrons will move from the n-type to the p-type, and holes will be moved from the p-type to the n-type, decreasing the number of charge carriers in this bulk of the silicon. This region, which has few charge carriers, is called the depletion zone. This smaller amount of charge carriers will make any signal generated by ionizing particles easier to detect. Silicon pixels are typically applied with a reverse bias voltage so that if an electron is ionized, the electron moves toward the n-type side while the hole moves toward the p-type side.

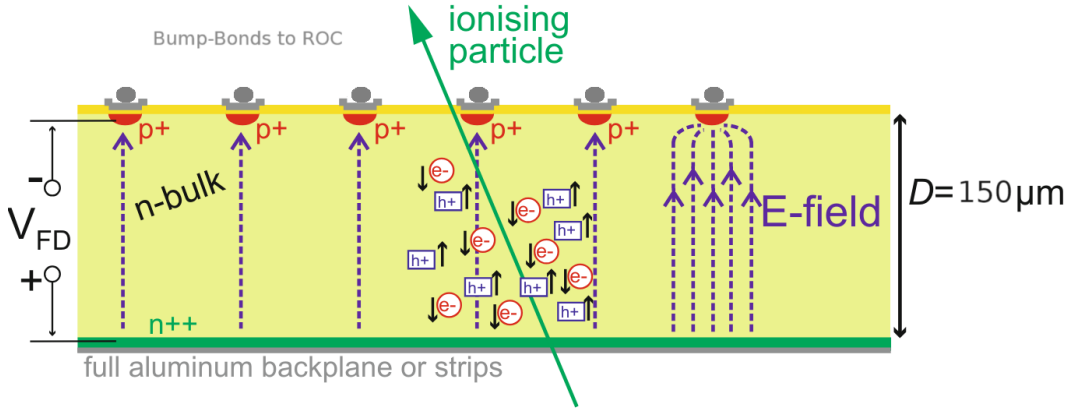

Figure 1: This figure shows a close-up image of a silicon pixel with an ionizing particle traveling through the n-type bulk, creating holes and electrons in its path. The electrons, due to the reverse bias, travel towards the n++ backplane, and the holes travel towards the p+ implants. This image is a modified version of one in Frank Hartman's book Evolution of Silicon Sensor Technology in Particle Physics[3, p. 24]

There are two types of silicon pixel sensors: 2D sensors and 3D sensors. For example, a p-in-n type 2D sensor has a large n-doped silicon substrate, an even more doped n++ backplane, and p-type implants on the opposite side, as seen in Fig. 1. For a 2D sensor, when a particle has ionized an electron from the bulk n-doped silicon, the particle starts to move in the direction of higher voltage towards the n-type side. In comparison, the hole moves toward the lower voltage towards the p-type implants. Assuming the pixels are 50μm by 50μm by 150μm, holes are equally likely to form anywhere in the substrate, and the path they take is a direct path to the implant. The average distance traveled by the holes is approximately given by this formula:

$$\int_0^{150}\int_{-25}^{25}\int_{-25}^{25}\frac{\sqrt{x'^2+y'^2+z'^2}}{50*50*150}\,dx'\,dy'\,dz' = 79.3\mu\text{m}$$

Therefore, the distance holes must travel is, on average, about 79μm. This is an approximate model of what is occurring in the sensor since there are other effects to create a signal, called the Shockley-Ramo theorem. Assuming our model holds once the charge carrier meets the implant or backplane, the produced current goes through a

bump bond to the CMS readout chip (CROC) to analyze the pulse of the current and determine whether it counts as a hit.

This average distance the holes travel, being about half the width of the card, means they are likely to run into traps as the sensor continues to be irradiated. As the sensor is irradiated, incoming particles can have enough energy to affect the atoms in the bulk silicon lattice by the electromagnetic or strong field, depending on your source. These impurities in the lattice can act as traps for the charge carriers, trapping more negative electrons on the n-type side, and positive holes are trapped on the p-type side. To counteract the charge buildup and ensure newly generated charge carriers travel in the correct direction, the reverse bias voltage must be increased to increase the electric field in the substrate.

CMS Readout Chip

Once an ionizing particle hits the sensors and the charge carrier has traveled to the bump bond, the current is passed to the readout chip. The CMS readout chip (CROC) must amplify this signal and check if it is above a certain threshold. If it is above this threshold, the CROC counts that as a hit and passes the data onto the High-Density Interconnected printed circuit board (HDI) for data collection.

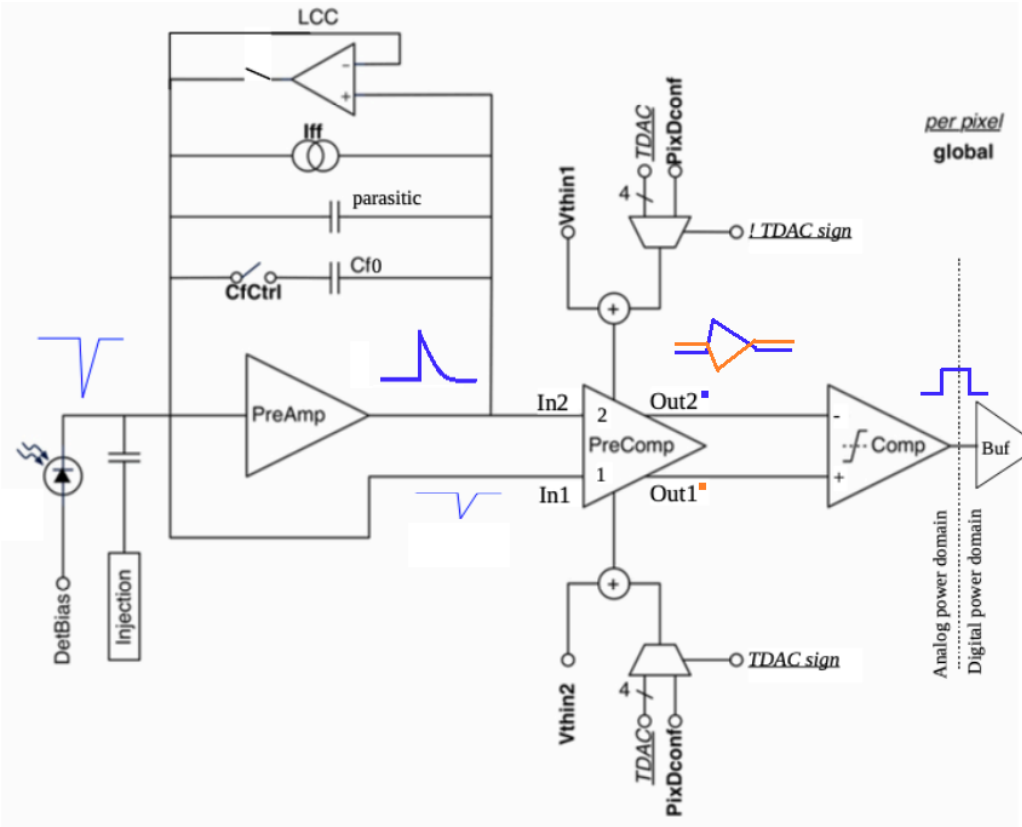

Figure 2: This figure shows how a signal sent from the silicon pixel would be altered by the analog front end to create a digital signal. The altering of the signal is largely influenced by the GDAC and TDAC registers as shown in the image. This was altered from an image used in Daniel Antrim presentation[1]

The first responsibility of a readout chip is to magnify the signal produced by the sensor pixel. This is first achieved using a pre-amplifier, as shown in Fig. 2. The output signal is both inverted and has a much stronger signal, so we can use it to determine if an ionizing particle was present. This has a feature that makes the discharge current constant rather than time-varying. After the signal has passed the pre-amplifier, the amplified signal passes onto the pre-comparator.

The Pre-Comparator prepares the signal for the comparator by amplifying the signal of the inverted signal and the original based on two registers, GDAC and TDAC. GDAC allows us to center the data of all the pixels around a certain threshold. While TDAC allows us to try to center individual pixels close to one threshold taking into

account minor differences between the pixels. The outputted data is then passed to the comparator.

The comparator is the final part of this simplified image of the CROC. The comparator takes these amplified signals and amplified inverted signals and compares them by checking when the noninverted signal is greater than the inverted signal, generating a time-over threshold signal which is then digitized, buffered, and sent out to be analyzed off the CROC.

From there, we can get an image of where ionizing particles likely went through the sensor. Combined with data from many sensors in the inner and outer trackers, we can reconstruct the path of particles and determine their charge and momentum. This all requires transferring data to computers and storing it to be analyzed utilizing HDI PCBs.

Communicating with the CROC

The CROC requires many registers to be set and many signals to be sent out for analysis/storage. Because of the inner tracker's space constraint, a High-Density Interconnected (HDI) printed circuit board is required. These boards allow many CROC Sensor assemblies to be wire-bonded to the HDI and used in unison. However, our experiment used a single chip card (SCC), which allowed us to run and collect data from a single CROC.

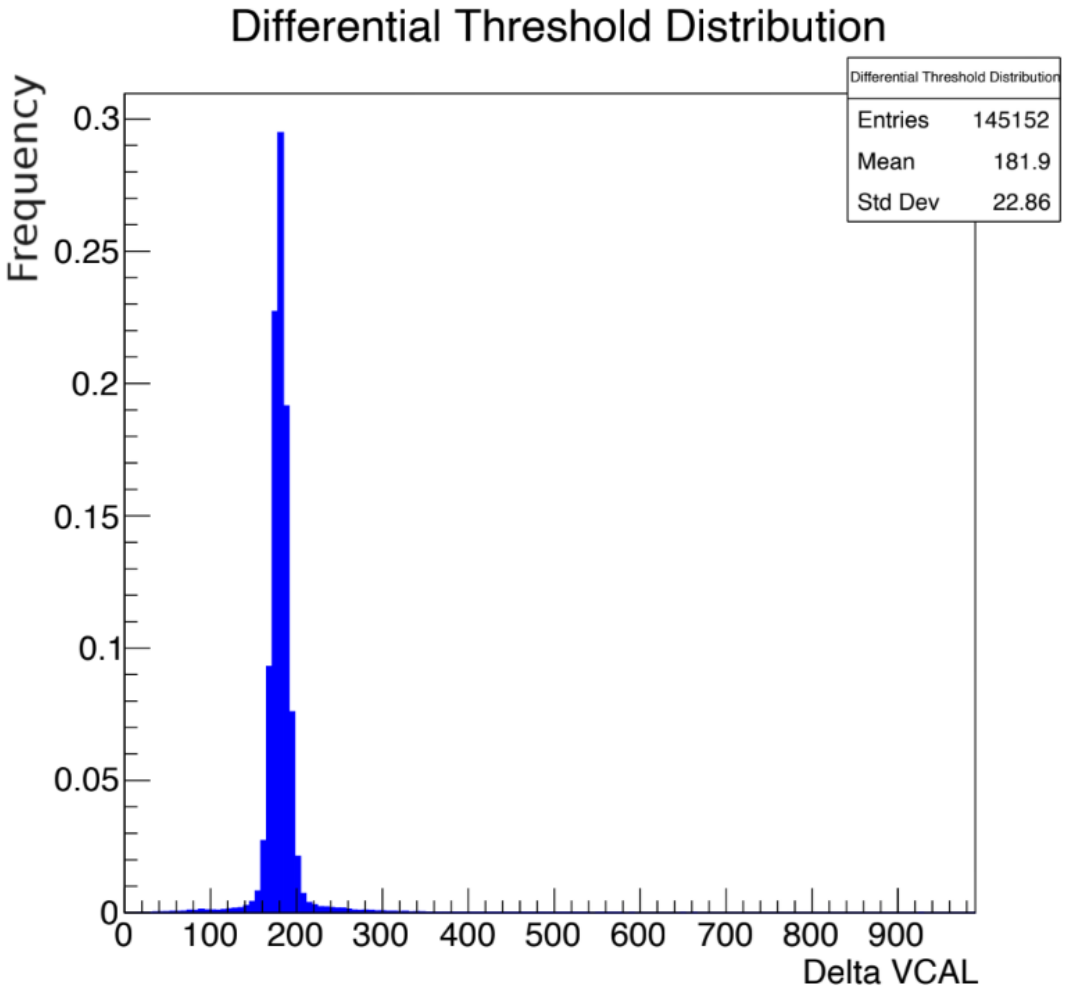

Figure 3: This figure shows the threshold distribution only about 24 MRad into our irradiation. This distribution has some significant tails due to not tuning LDAC too much by this point in the irradiation.

This SCC utilizes a Display port for some communication with a computer on the outside. When the card is powered, this display port allows us to configure the CROC with the voltages and run scans such as a Threshold Scan to receive data on the CROC's Threshold distribution when we inject charge into the analog front end of the CROC, an example is shown in Fig. 3. We can also set voltages such as GDAC to control the overall threshold of the pixels and TDAC to change individual pixels to center the thresholds. Not all data can be acquired via the display port but requires another input to SCC called a MuxScan.

The MuxScan, short for multiplexer scan, requires another input signal to tell the card which voltage to output. This output voltage is returned after the card receives the input signal, which returns the desired voltage. Some of these voltages describe the temperature and radiation dose the CROC has received using the temperature and radiation effects on two types of transistors. Other voltages describe details on how the card is configured, like the voltage the card sees from the inputs and internal voltages like GDAC. Some of these voltages are extremely temperature sensitive, which is one reason for keeping the temperature as constant as possible.

Methods

The Irradiation

We irradiated a CROC with no sensor on an SCC at Sandia National Lab in Albuquerque, New Mexico, with a Co60 gamma-ray source. We hoped to look for any irradiation effects and compare them to an X-ray irradiation performed by another CMS group. Irradiation has been known to affect transistors, of which the CROC has many. In the past, we also have seen wire bonds become damaged through the process of irradiation, which a couple of possible effects can cause. Any other irradiation damage to the CROC is important to learn about to ensure the chip can last at least five to ten years in the experiment depending on where they are positioned on the beam line.

Experiments on the card have been performed using a highly columnated X-ray source on mainly just the CROC, but the cards in the experiment won't just have energies in the X-ray range during eventual data taking, but will also see energies in the Gamma photon range as well. To irradiate with gamma rays, we used a Co60 source, which decays mostly by releasing a .31 MeV beta-particle, which changes the Co60 into an excited Ni60. The Ni60 then, to reach a ground state, releases 1.17 MeV and 1.33 MeV gammas. There is another decay of the Co60, which produces a 1.48 MeV beta particle. However, this only happens once for every 830 .31 MeV beta decays, therefore, the one decay can describe most of the irradiation. Because a layer of metal can mostly stop beta particles, the beta particles should be stopped by the thermos holding the CROC. The gamma rays that make it through are well above the energy required to ionize electrons within the electronics.

The ionizing radiation can affect the card in many ways, such as altering the properties of transistors and damaging the material the card is made of. As the ionizing particles go through the silicon, they can move atoms from their positions in the lattice. The displaced atoms can now occupy different energy levels in the silicon, which changes the properties of the transistors. Once this changes the properties of the transistors, the CROC/SCC will behave differently. On top of this, ionization energy can damage the

CROC and SCC materials.

Damage to the card's material can make the card brittle and eventually break parts such as wire bonds. In the past, we have noticed damage to the wire bonds connected to the wire bond pads of the card. This was thought to possibly be due to outgassing, where material inside the card becomes gaseous, breaking down the material in the card. Halogen elements in the card were thought to be the source of this outgassing, so a halogen-free card was used, as well as a cover that allowed gas not to be trapped next to the wire bonds.

Radiation can damage cards in many ways, which can affect them in unpredictable ways. Damage to the transistors and the wire bonds can change the card's behavior, making the card behave differently, and eventually stop working altogether. We have made steps to reduce damage to the wire bonds by using a halogen-free board and a cover that allows gas to flow away from the card. During the irradiation, we constantly recorded the supply voltages every 10 minutes, ran MuxScans and ring oscillator scans every 15 min, and tuned the card occasionally to center the threshold distribution of about 1000 electrons. All of these scans are affected by the irradiation of the card with gamma rays.

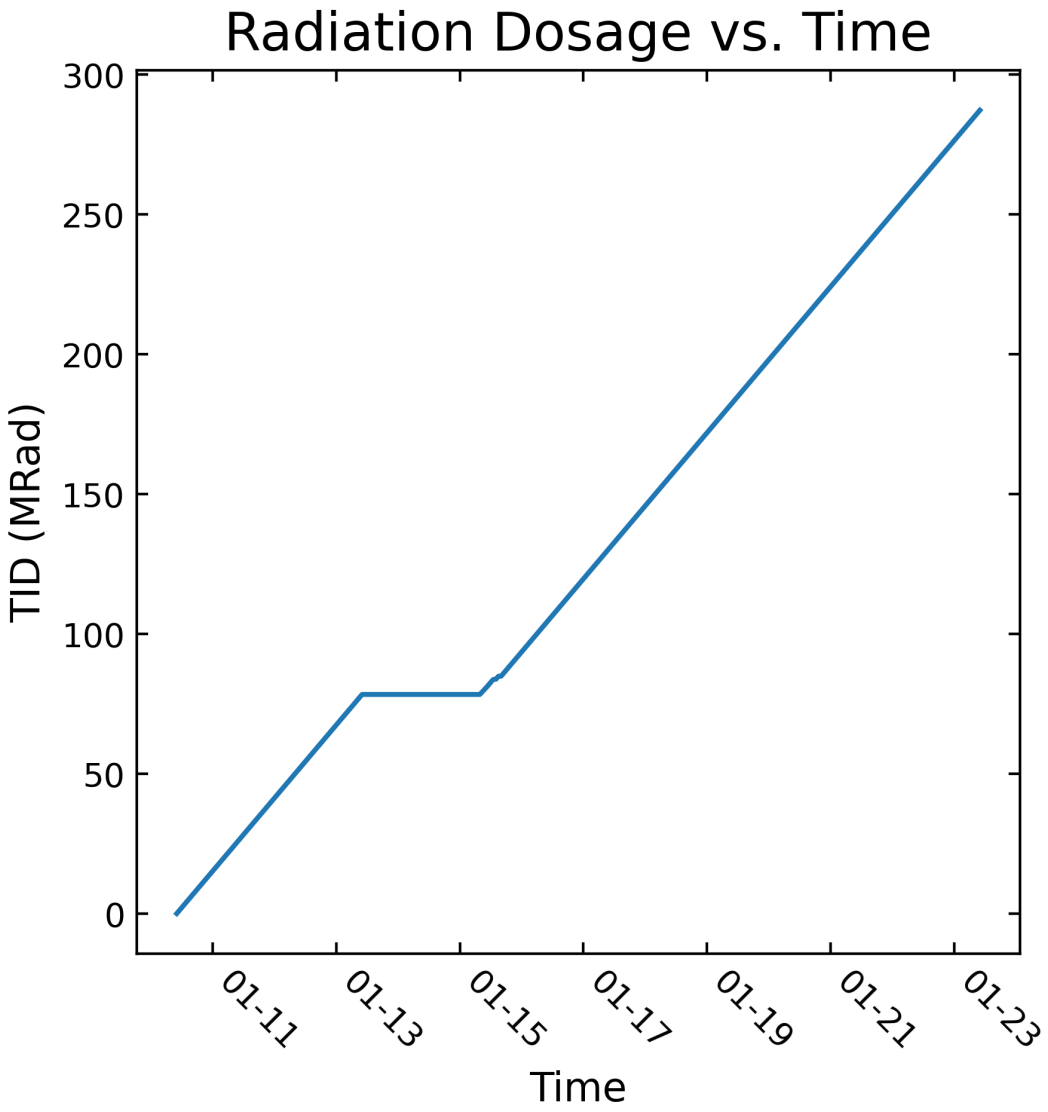

Figure 4: This figure shows our accumulated dose as a function of time over the course of the irradiation. The first flat part was due to the irradiation being set on a three-day timer and stopping at some point over the weekend. There are also a couple of bumps on the fifteenth where we brought the source back down to troubleshoot

To relate the CROC damage to the amount of radiation dose the card receives, we need to know the dose as a function of time. Ionization chambers can measure the dose rate at a position. However, the ionization chamber can only be used before or after the irradiation, and the dosage is calculated afterward. After the irradiation, we used an ionization chamber and measured the dose rate to be 302.14 rad/sec. With this dose

rate, we could calculate the function of dose vs time, including the times when the source was taken away due to technical difficulties. This would allow us to plot any voltages we read of the card vs. dose. The function of Total integrated radiation dose vs. time is shown in Fig. 4, and you can see the flat areas where the source went down over a weekend, but at the end of the irradiation, we were still able to get up to 287 MRads of dosage.

Temperature Control

During the irradiation, we need to keep the temperature as close to -20 degrees Celsius as possible. This is because in the CMS experiment, the electronics will be kept at -20 Celsius, and the irradiation effects can be annealed from the material by raising the temperature. To do this, a previous undergrad Honors student working in the lab, Colin England, set up a cooling system to control the temperature with good precision using forward extrapolation.

We have a system that relies on liquid nitrogen boil-off to control the card's temperature. The accurate temperature measurement required is from a thermo-couple in thermal putty between the SCC and its heat sink. The cooling system has a small dewar filled with liquid nitrogen, aswell as a resistor pack. Current flows through the resistor pack, which we control with a computer and power supplies. The resistors heat up as current passes through them. The created heat, in turn, boils some of the liquid nitrogen. This boiled-off, now gaseous, nitrogen is still very cold and moves down a transfer line to a thermos containing the card by the cobalt 60 source. This cold gas moves around the card, cooling it off and flows over the CROC, hopefully reducing the risk of outgassing. The use of a nitrogen cooling system has its benefits, one of which is the environment in the thermos is very dry, so ideally no water builds up on the electronics. This setup controls the temperature very well if it weren't for the fact we need to fill the small dewar occasionally when we run low on liquid nitrogen.

Filling the small dewar with liquid nitrogen, what we will call autofills, forces

gaseous nitrogen to flow down the transfer line quickly, which drops the temperature. This pressure wave of cold gaseous nitrogen was mitigated by using a gravity feed, which allows the liquid nitrogen to fall slower than if we had directly filled the dewar. Even with the gravity feed, we still see dips from -24 degrees Celsius to -26 degrees Celsius. The bigger issue is when it is below temp, the current is not flowing, which in the past would cause the transfer line to warm up, and when we wanted to cool the thermos, it would take a while for the thermos to start dropping in temperature. When the thermos finally started cooling, the temperature have been up to -14 degrees Celsius or worse. This was resolved by Colin England and me, making the system turn on the current when the rate of increase in temperature was too large.[2] This worked great, and we no longer saw any overshooting of -20 Degrees Celsius.

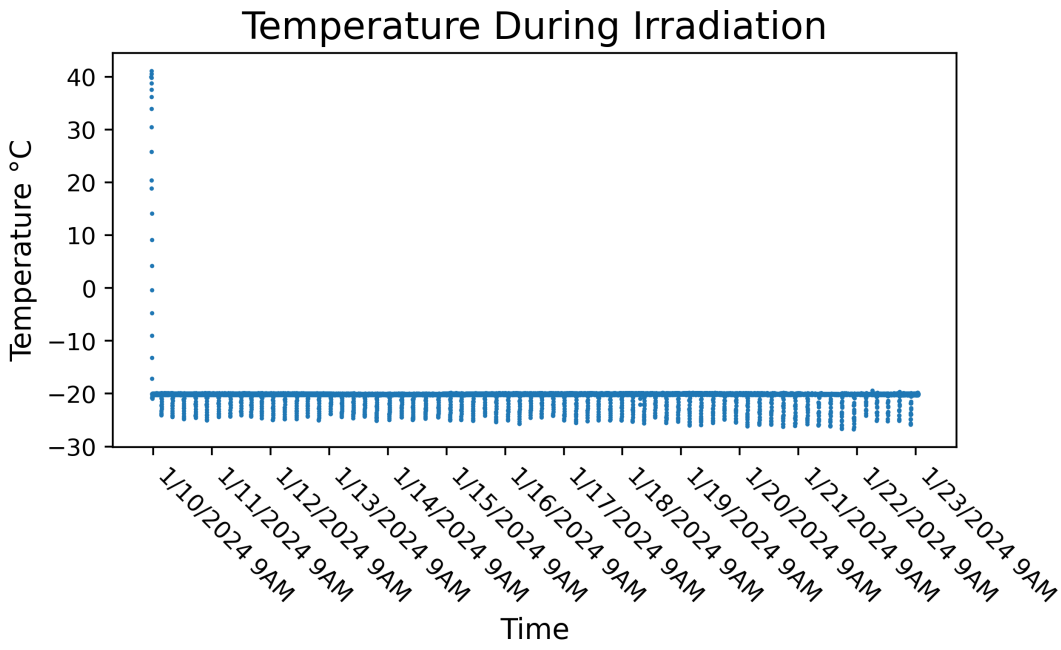

Figure 5: This is the temperature over the full irradiation. The irradiation started shortly after the temperature dropped down to -20 at the start. The periodic dips down are due to the autofill turning on to fill the small dewar

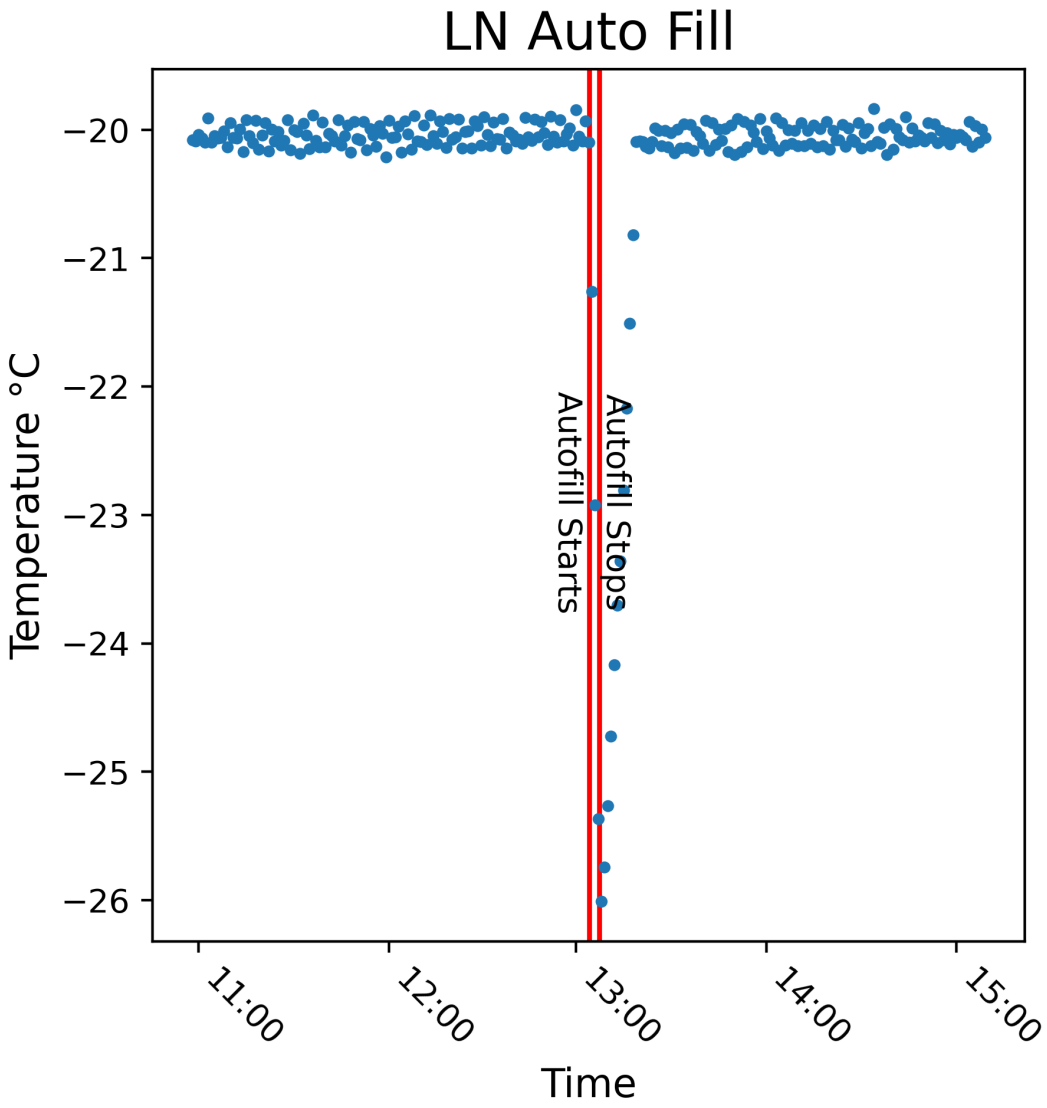

Figure 6: This figure shows a zoomed-in plot of the temperature over one period of the autofill period. The autofill starting and stopping are shown by the red lines. The temperature before and after the autofill is held very close to -20 Celsius

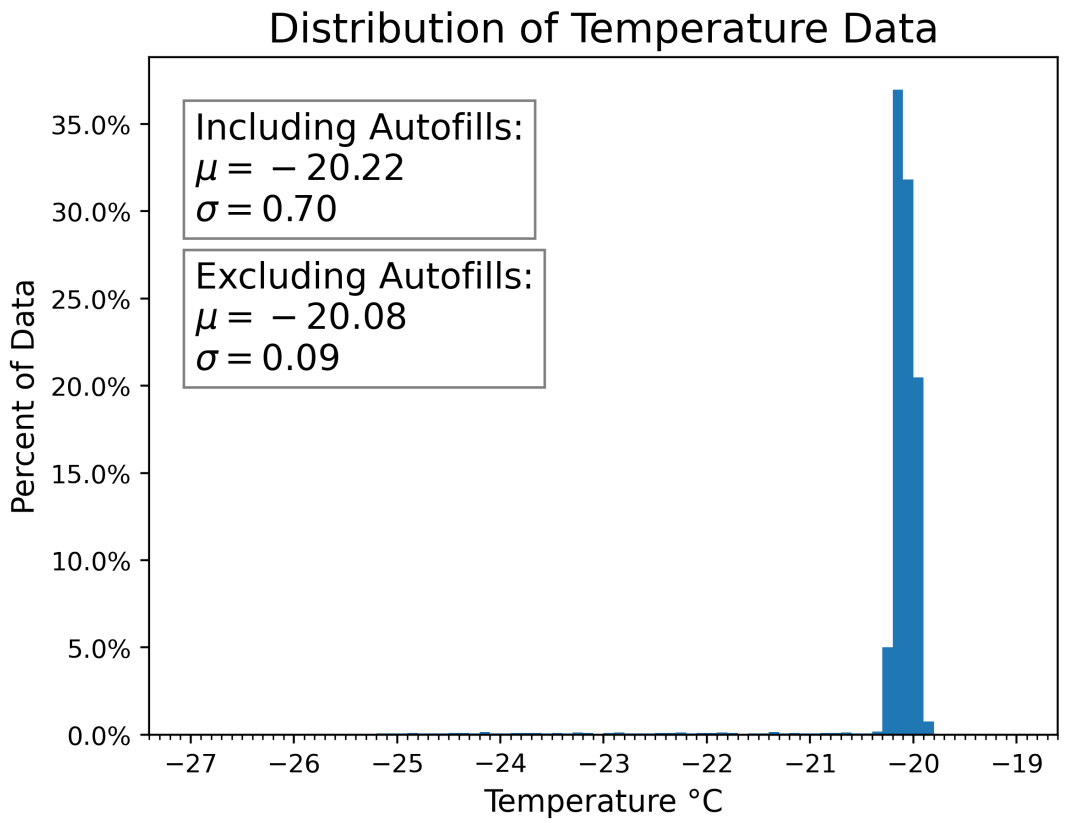

Figure 7: This figure shows the distribution of the temperature of the system. Along side this the mean and standard deviation are shown including the autofill data and excluding the autofill data.

Thanks to Colin England, we were able to control the temperature very well. The CROC stayed around -20 degrees Celsius for most of the irradiation except for the occasional autofill, which still brings it down to -24 to -26 degrees Celsius, as you can see in Fig. 5 aswell as Fig 6. The temperature distribution(Fig. 7) shows us especially when there were no autofills, we were able to control the temperature very well. Therefore, we did not anneal any of the damage to the electronics during the irradiation, and we were able to keep the electronics in a similar environment to what would be expected in the cold environment of the CMS experiment.

Results

VMUX

VMUX Name	γ-ray Irradiation Percentage Change at 287 MRad	X-ray Irradiation Estimated Percent Change at 287 MRad
GDAC_L	+5.2	+10
GDAC_M	+8.1	+13
GDAC_R	+7.3	+13
RADSENS_ACB	-1.4	-2
RADSENS_SLDOA	-1.5	-2
RADSENS_SLDOD	-1.4	-2
RPOLYTSENS_BOTTOM	+4.3	+4
RPOLYTSENS_TOP	+5.0	+4
TEMPSENS_ACB	+1.0	+2
TEMPSENS_SLDOA	+1.0	+2
TEMPSENS_SLDOD	+1.0	+2
VCAL_HIGH	+1.5	+8
VCAL_MED	+1.3	+4
VDDA_HALF	+0.1	$\approx$0
VDDD_HALF	+2.1	$\approx$0
VINA_QUARTER	-3.0	-2
VIND_QUARTER	-0.4	$\approx$0
VOFS_QUARTER	+1.0	+5
VREFA	+0.4	$\approx$0
VREFD	+2.1	$\approx$0
VREF_ADC	+1.2	+8
VREF_CORE	-0.2	+3
VREF_KRUM	+6.5	+13
VREF_PRE	+0.4	+10
VREF_VCAL_DAC	+1.4	+8

Table 1: The percent change of the MuxScan voltages for the voltage values in the chip. The γ-ray data is calculated using the data from the irradiation while the X-ray values are approximated by Alkis Papadopoulos talk.[5]

IMUX

IMUX Name	γ-ray Irradiation Percentage Change at 287 MRad	X-ray Irradiation Estimated Percent Change at 287 MRad
CDR_CP	+3.1	+8
CDR_CPBUFF	+1.5	+5
CDR_CPFD	+2.5	+9
CDR_VCO	+2.3	+9
CDR_VCOBUFF	+3.1	+4
IINA	+3.0	+18
IIND	+1.4	+2
I_PREAMP_L	+1.7	+7
I_PREAMP_M	+0.2	+10
I_PREAMP_R	+2.8	+7
I_PREAMP_T	+1.8	+9
I_PREAMP_TL	+3.1	+11
I_PREAMP_TR	+2.3	+10

Table 2: The percent change of the MuxScan voltages for the current values in the chip. The γ-ray data is calculated using the data from the irradiation while the X-ray values are approximated by Alkis Papadopoulos talk.[5]

Temperature Sensors

Measuring the temperature via the k-type thermos-couple is a very reliable temperature sensor even throughout irradiation, but the card also has built-in temperature sensors. Three built-in diode-connected CMOS transistors can be accessed using a MuxScan, and the MuxScans output a voltage that is related to the temperature of the card.[6] This can tell you the temperature of the card if it is calibrated correctly; because we were using the thermocouple, we didn't bother with the calibration. However, it is still interesting to compare it to the temperature measured from the thermocouple. On top of this, there are two other differential temperature sensors. These differential temperature sensors measure the difference in temperature across the chip using two temperature-sensitive resistors. This temperature sensor seems to be telling us a different story than many of the other voltages, with our change being twice that of the x-ray groups.

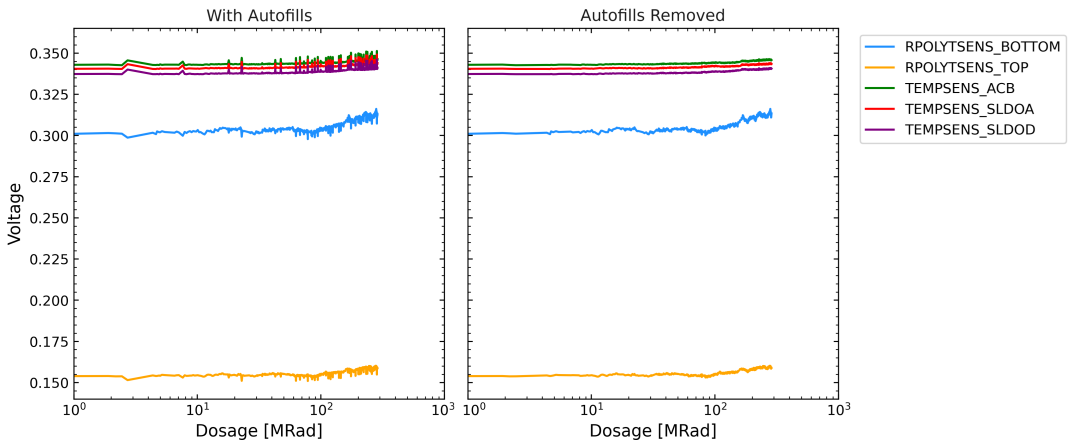

Figure 8: This figure shows the built-in temperature sensors on the CROC. The left has the autofill data included, while on the right, the autofill data (from the thermocouple) is removed. This shows that the temperature sensors were seeing the fluctuation in temperature due to the autofills.

The temperature sensors, as well as the differential, perfectly correlate with the temperature pulled off of the thermos-couple. The raw data from the temperature sensors is shown on the left in Fig. 8, while the data where the temperature(as measured by the thermocouple) was below -20.3 Celsius were removed on the right in Fig. 8. As you can see, the dips seen on left of Fig. 8 are completely removed on the right Fig. 8. Therefore, the temperature sensors seem to at least be outputting a voltage that is correlated with temperature changes.

When comparing our temperature sensor irradiation effects with that of the x-ray irradiation, we do see some differences. The output voltages are TEMPSENS_ACB, TEMPSENS_SLDOA, and TEMPSENS_SLDOD, which are positioned at different points on the chip. From Table 1, we see a 1.0% increase in the voltage over the irradiation, while the x-ray group saw about a 2% increase at this point in the irradiation in the voltages. It is unclear if this is significant, especially when you realize the x-ray irradiation was held at 10 degrees Celsius, but there does seem to be a smaller radiation effect on these voltages for the gamma irradiation.

The differential temperature sensor's outputs, RPOLYTSENS_BOTTOM and

RPOLYTSENS_TOP, seem to be larger for the gamma-irradiation than that of the x-ray irradiation. This differs from the other percent changes of voltages in Table 1, with our voltages changing more than those of the x-ray groups. However, whatever the cause, we care about the difference in the voltages. This difference has a smaller percent change of 3% for the x-ray irradiation and 4% for our irradiation.[6, p. 91] This means although our voltages drifted up more, the two voltages continued up at close to the same rate. This means the chip is telling us the temperature across the chip increased less for the x-ray irradiation than ours. This difference, however, is hard to tell if it is significant enough to say our chip behaved differently for these voltages.

Irradiation sensor

To compare the voltages from the x-ray group to our gamma irradiation voltages, we need to ensure we irradiate them with the same dose. We can measure the radiation dose with an ionization chamber or the Bipolar Junction transistors (BJT). However, to measure the approximate radiation dose with the BJTs, we can run a MuxScan to gather the voltage outputs of the radiation sensors. The radiation sensors are positioned near the same important parts of the chip as the temperature sensors, and they also consist of a transistor. However, these BJTs have the property that when it is being dosed with radiation, they behave predictably. These BJT changes during irradiation are relatively consistent as long as the temperature is held constant. This allows this transistor to be used as an approximate radiation sensor.

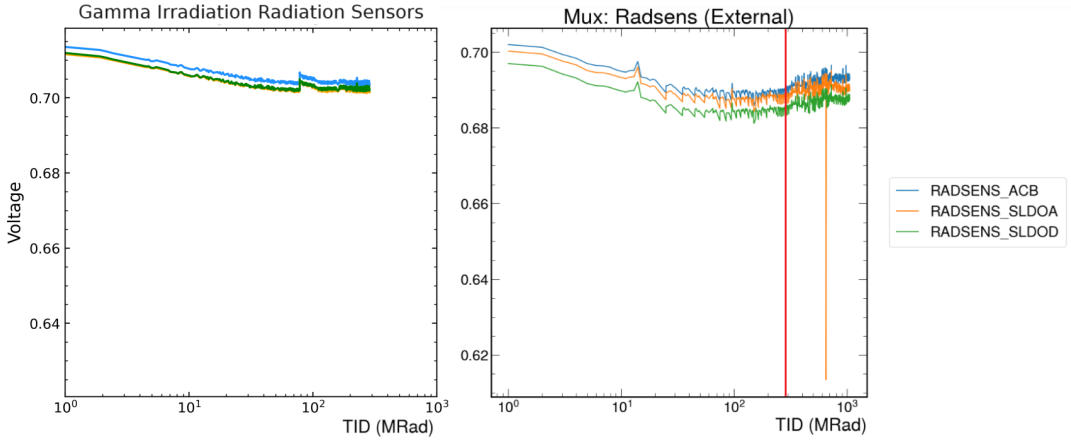

Figure 9: This figure shows the output voltages of the radiation sensors on the cards. The left is our gamma irradiation while the right is the X-ray irradiation. The red line on the right shows how far we were able to get in our irradiation.[5, p. 150]

The output of the three radiation sensors should be similar to that of gamma-ray irradiation and x-ray irradiation. The curves of both group's radiation sensor voltages are shown in Fig. 9. The curves do appear to have similar shapes up until 287 MRad, where we stopped our irradiation, and also at around 100 MRad, the bump you can see in the gamma irradiation is when the source was taken away, and the damage from the ionizing gammas started to anneal out of the BJT. The percent change for RADSENS_ACB, RADSENS_SLDOA, and RADSENS_SLDOD was -1.4%, -1.5%, and -1.4% for us, respectively, while the x-ray irradiation had about a -2% change when they had 287 MRad. This is interesting because their radiation sensor voltages dipped down and then came back up. Even though the X-ray plot does start moving upwards a little, and we don't see it on the gamma plot, It could be that we didn't irradiate to the point where the voltage starts moving upwards. The percentage changes of the RADSENS voltages are close enough to say these BJTs agree with the ionization Chamber.

Input Voltages/Currents

Running the CROC requires a supply of a voltage for the analog and a voltage for the digital to the card, which, using a voltage regulator, powers the chip and card. We were able to measure the input voltages and currents in two ways: a script measuring the voltage on the supplies every 10 minutes from the supplies, as well as from the card that returns voltages in the MuxScan every 15 minutes. The x-ray irradiation showed a large increase in the analog current, which we saw as smaller.

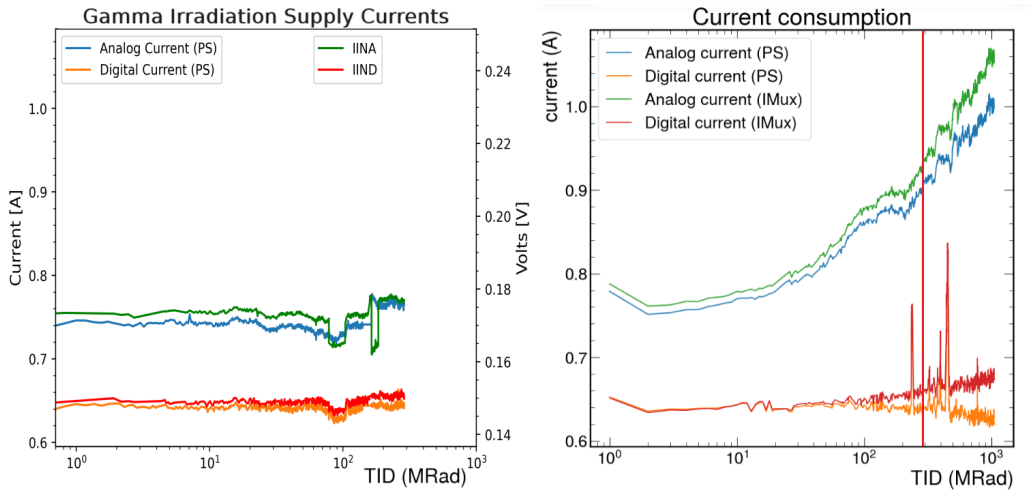

Figure 10: This figure shows the currents powering the card as measured by the card and the power supply. The left is our gamma irradiation, while the right is the X-ray irradiation. The red line on the X-ray plot shows how much total dose were were able to apply compared to their dose. This was made using data from the X-ray irradiation's presentation [5].

The input currents from the X-ray irradiation and our gamma irradiation seem to have some differences. From Fig. 10, you can see the input currents for both the gamma irradiation and the x-ray irradiation, which are measured through the power supply and the MuxScan. The voltages IINA and IIND are proportional to the analog current input and the digital current input as measured by the card. Both of their currents seem to have a large change over the course of the irradiation. Their analog current percent change from the start to when we stopped at 287 was about 16% and 18% as measured by their

power supply and their MuxScan, respectively. When we look at ours, we saw 4.5% and 3.0% increases, respectively. For the digital currents, we also see larger changes for the x-ray irradiation, with theirs increasing about a percent change of -2% and 2% for the power supply and MuxScan, respectively, while ours was -0.3% and 1.4%, respectively. They experienced the analog current increasing at a fast rate while we saw half the percent change that they saw. There is another difference in the plots at about 100 MRad and 200 MRad our currents seem to fluctuate but this is due to issues with the irradiation stopping and our power supplies having issues. This is talked about more in the VINA discussion in the External Voltages section. This could be an effect of different sources affecting the electronics in different ways or the cards breaking in different ways.

Whatever the cause of this different behavior, our behavior seems a little better than theirs during the irradiation. The cause of this is not definitive. However, in the x-ray irradiation presentation, they mentioned two campaigns that showed a 5% increase in analog currents while two others showed a 20% increase in analog current over the full 1Grad.[5] Because we didn't go to 1 GRad, we cannot say for certain if our CROC would have gone to a 5% or a 20% increase in analog current.

External Voltages

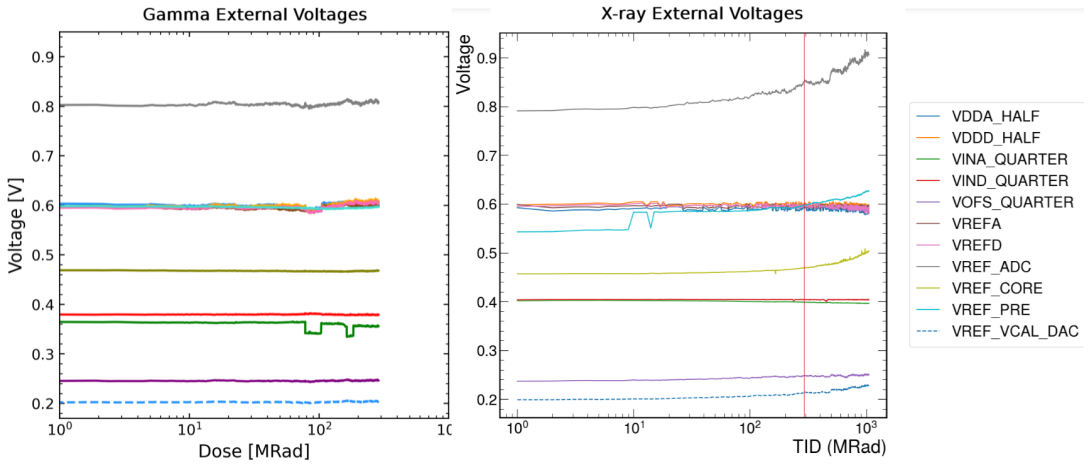

Figure 11: This figure shows the external voltages of the card outputs. The left is our gamma irradiation while the right is the X-ray irradiation. The red line on the right shows how much dose we were able to achieve compared to how much the X-ray group was able to achieve. This was made using images from the X-ray group's presentation[5].

There are a large number of other voltages which we can pull from the MuxScan. These tell us what the CROC's voltages are. Some of these voltages are GDAC, which controls the global threshold around which the CROC is centered. There is also the voltage that the CROC sees at the regulator, which is called VINA and VIND. Another very important voltage is also VREF_ADC, the analog-digital converter, which, if broken, the CROC stops sending out data because it would no longer be able to convert the analog signal to a digital signal. Lastly, there is one important voltage that does change more in ours than it does for the x-ray groups, but this can be explained by our different approaches. The trend of the x-ray group voltages increasing more than ours or changing similarly to ours seems to continue with the external voltages.

GDAC, being a voltage that controls the centering of the threshold distribution, means GDAC is a voltage we want to be able to control at all times. The difference in GDAC between the x-ray irradiation and our gamma irradiation is substantial. GDAC_L, GDAC_M, and GDAC_R for the x-ray group changed by 10%, 13%, and 13%, respectively. While ours only changed by 5.2%, 8.1%, and 7.3%, respectively, the x-ray group's

voltages seem to be increasing by twice as much as we had to change ours.

This discrepancy between our irradiation and the x-ray irradiation makes it seem like we are dosing our CROC with a smaller dose, but we know we are irradiating it with the same radiation dose. This, in part, could be explained by the fact that the X-ray group is dosing unevenly. This could make the thresholds more spread out and may have an effect on what you have to set GDAC at. However, there is not enough data to say for sure what this effect is

VINA and VIND are the voltages the CROC says it is being powered with, which makes these important for seeing how much power the CROC is using and how it increases with dosage. This voltage change during the x-ray irradiation matches the voltage change we saw in the gamma irradiation. We both saw a small change in the digital voltage of about less than .5% change for the x-ray group and -.4% change in the gamma irradiation. The analog voltage also changed similarly, with the x-ray irradiation changing about a -2% while we saw a -3% change as well. In Fig 11, you can see our VINA does move around a bit. The first dip is due to the VINA starting to creep down when the irradiation stopped we are not sure if these events are related. We didn't correct the input voltage till we noticed later on. then the power supply froze and was brought back at the incorrect voltage till it was eventually corrected later on. This fluctuation during the irradiation is not a result of the CROC behaving strangely but technical difficulties with the power supply. However, the total changes in VINA and VIND show that even though we do see a lot of differences between our irradiations, we do have the same change in how much voltage the CROC is being powered with.

The other voltage that is important in this group of voltages is the VREF_ADC, which is the voltage at the analog-digital converter. Being able to control this component is vital to communicating with the CROC. The x-ray groups VREF_ADC did change by about 8%, while ours only changed by 1.2%. Again, the X-ray group's voltage changes by a larger percentage than ours. These large changes seem to show that our irradiation seems to be affecting the CROC in less extreme ways, but there is no definitive answer

for why.

You may have noticed that the voltages VDDD and VDDA have a larger percentage change for the gamma irradiation. A large percent change is expected because the regulator that controls VDDD and VDDA requires trim bits to be set to ensure that VDDA_HALF and VDDD_HALF are equal to .6, which is the optimal voltage the system should run with. While the x-ray group updated the trim bits throughout the irradiation, we updated them once at just about 100 MRad, where you see the voltages jump up closer to .6 Volts. Their constant updating of the trim bits ensured that the percent change in VDDD and VDDA was near 0 while our percent changes were allowed to creep up as the irradiation continued.

The external voltages show that as the CROC is being irradiated, some voltages seem to be changing similarly to the changes we see. However, others are drastically different, with the percent changes being factors of two or more larger for those of the X-ray irradiation. Most of the MuxScan voltages shown in Table 1 and Table 2 are either similar or have the voltages from the X-ray irradiation changing by at least factors of two more than our voltages changed.

Ring Oscillators

The ring oscillator scan can be performed, which returns the count of how many times a ring oscillator switches on stored in a 12-bit register, which is returned by the scan. The purpose of the ring oscillator is to determine the radiation damage effect on the logic cells of the chip [6, p. 92]. Damage to the logic cells can affect how fast the ring oscillators oscillate. This, in turn, affects how many oscillations the ring oscillators can achieve. The different enable signals are shown in Table 3, with different logic cells that make them up. Our results for these values differ largely from those of the X-ray groups.

Bank	Type	Group
A	Strgth. 0 inv. clk. drvr.	0
A	Strgth. 4 inv. clk. drvr.	1
A	Strgth. 0 inverter	2
A	Strgth. 4 inverter	3
A	Strgth. 0 4-input NAND	4
A	Strgth. 4 4-input NAND	5
A	Strgth. 0 4-input NOR	6
A	Strgth. 4 4-input NOR	7
B	Strgth. 0 inv. clk. driver	B-left, B-right
B	Strgth. 4 inv. clk. driver	B-left, B-right
B	Strgth. 0 inverter	B-left, B-right
B	Strgth. 4 inverter	B-left, B-right
B	Strgth. 0 4-input NAND	B-left, B-right
B	Strgth. 4 4-input NAND	B-left, B-right
B	Strgth. 0 4-input NOR	B-left, B-right
B	Strgth. 4 4-input NOR	B-left, B-right
B	Strgth. 0 scan D-flip-flop	FF
B	Strgth. 1 D-flip-flop	FF
B	Strgth. 1 Neg. edge D-flip-flop	FF
B	Strgth. 0 LVT inverter	LVT
B	Strgth. 4 LVT inverter	LVT
B	Strgth. 0 LVT 4-input NAND	LVT
B	Strgth. 4 LVT 4-input NAND	LVT
B	Strgth. 4 inj-cap-loaded 4-input NAND	CAPA

Table 3: These describe the logical components of the ring Oscillator circuits. The ones in the same group can only be run simultaneously. Strgth. refers to the size of the transistor (0,1,4). The unirradiated CROC has approximately 600 MHz frequency signals from Bank A Ring Oscillators and 800 MHz frequency signals from Bank B Ring Oscillators.[6, p. 121]

The relative change percentage tells us if the ring oscillator has slowed compared to the unirradiated CROC. Fig. 12 shows the Relative change percentage, which allows us to compare how our oscillator evolves during the irradiation. An increase in the ring oscillator counts can mean that the logic of the control signals has slowed, and a decrease in the ring oscillator counts can mean that the Ring oscillator logic cells have slowed down. However, It can also mean other effects are taking place, such as losing the voltage in the enable signal or losing the voltage in the ring oscillator circuit. We can see that the x-ray irradiation and our gamma-ray irradiations do agree that the counts increase at first for all of them, and then they start to decrease over time. However, the average relative

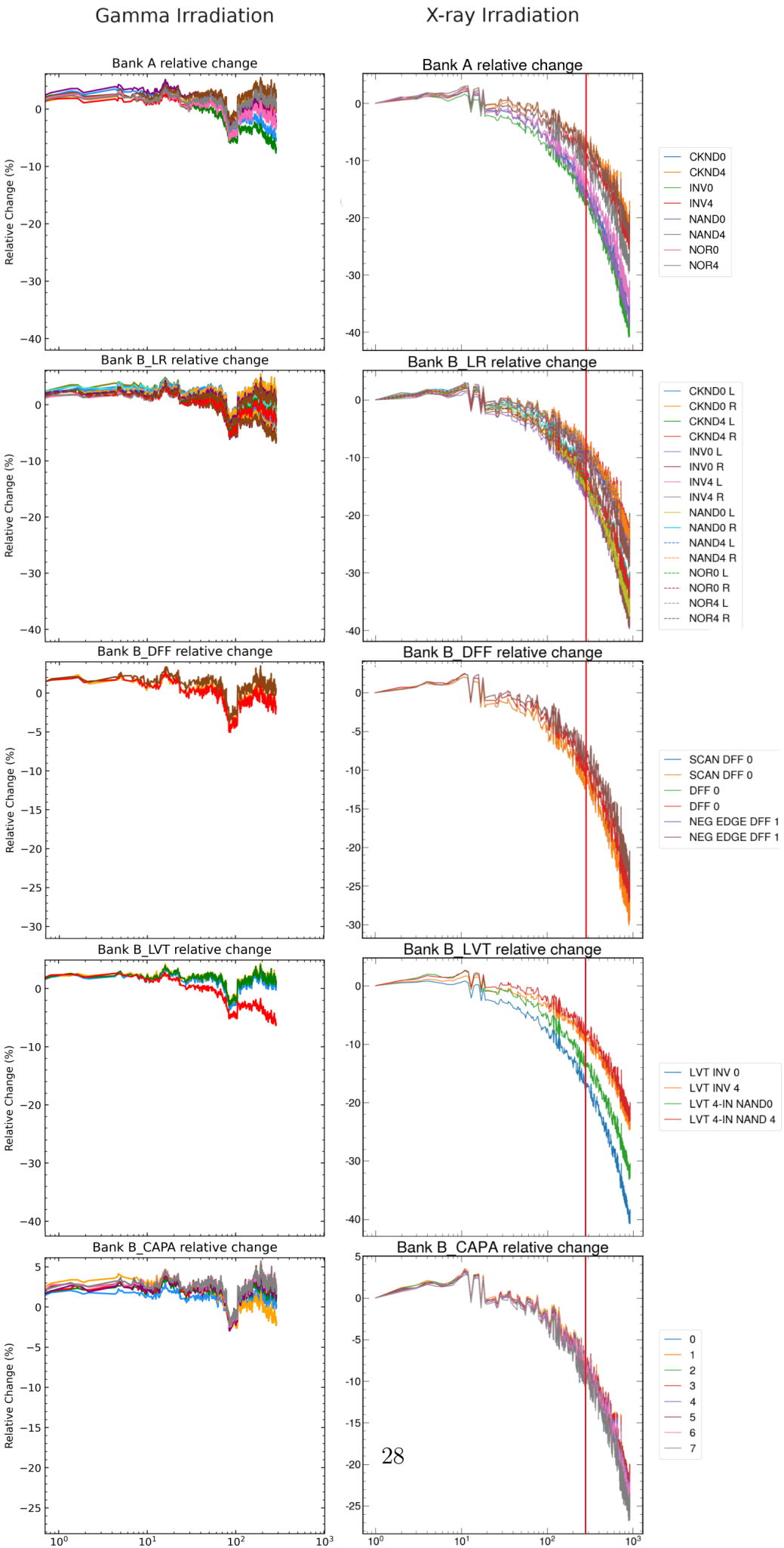
Gamma Irradiation
X-ray Irradiation
Bank A relative change
Bank B_LR relative change
Bank B_DFF relative change
Bank B_LVT relative change
Bank B_CAPA relative change
Relative Change (%)
CKND0
CKND4
INV0
INV4
NAND0
NAND4
NOR0
NOR4
CKND0 L
CKND0 R
CKND4 L
CKND4 R
INV0 L
INV0 R
INV4 L
INV4 R
NAND0 L
NAND0 R
NAND4 L
NAND4 R
NOR0 L
NOR0 R
NOR4 L
NOR4 R
SCAN DFF 0
SCAN DFF 0
DFF 0
DFF 0
NEG EDGE DFF 1
NEG EDGE DFF 1
LVT INV 0
LVT INV 4
LVT 4-IN NAND0
LVT 4-IN NAND 4
0
1
2
3
4
5
6
7

change percentage for x-ray irradiation has the Bank A, Bank B_LR, Bank B_DFF, Bank B_LVT, and Bank B_CAPA counts changing about -12%, -12%, -9%, -11% and -8% on average respectively while ours changed -1.5%, -1.3%, -1.0%, -0.7%, and +1.5% on average respectively. These changes show that the X-ray irradiation saw a large decrease in the counts throughout the irradiation. At the same time, our Oscillators kept recording almost the same number of counts over the whole irradiation with very little radiation damage to the logic cells.

There is a large decrease in the number of counts over the course of the irradiation for the x-ray irradiation, which can mean a couple of things that could cause the ring oscillator to slow down or the enable bit signal to lose its voltage faster. Either way, x-ray irradiation saw a larger amount of radiation damage to the logic cells, while our gamma irradiation saw very small damage to the logic cells of the circuit.

Tuning Results

During the irradiation, we occasionally have to perform threshold tuning. This is done by performing three scans, GlobalThresioldTuning to tune GDAC so the threshold is about 1000 electrons. ThresholdEqualization tunes the TDAC values so the distribution is not spread out, while ThresholdScan, which returns what the threshold distribution is, is by injecting the pixels in the CROC with charge. On top of this, LDAC is another register you can change, and changing LDAC can change how many pixels are in the tails of both the TDAC distribution and therefore the tails of the threshold distribution. All of this is to tune the threshold distribution to as close to 1000 electrons.

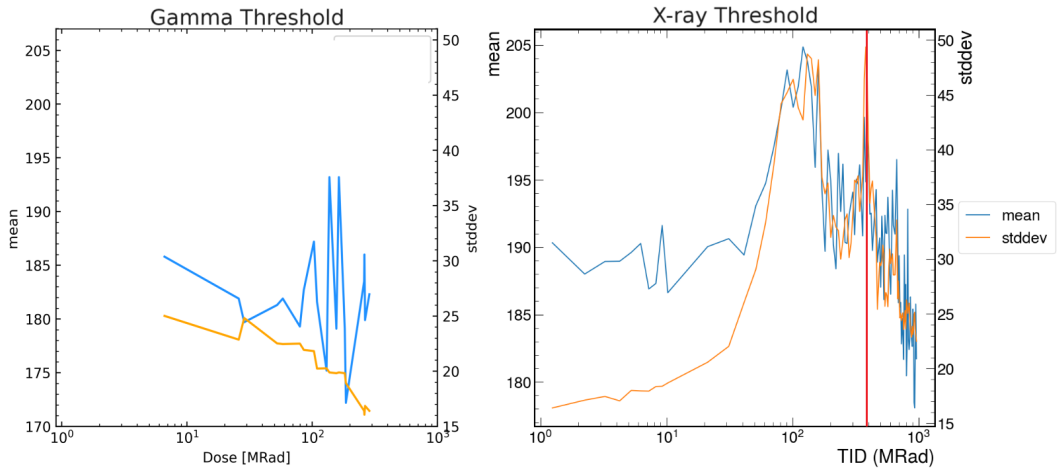

Figure 13: This figure shows how the mean and standard deviations changed during the irradiation. The left is our gamma irradiation results, while the right is the X-ray results. The red line on the right plot represents how much total dose our CROC received.[5]

Our threshold tuning increased as the irradiation continued. The steady decrease in the standard deviation during the irradiation is shown in Fig. 13. As the irradiation continues, you would expect the behavior to be less well-defined, so the standard deviation of the threshold distribution should increase. However, our increase is not the result of the electronics somehow behaving more predictably but rather Jesse Harris tuning the CROC extremely well. To start the irradiation, we hadn't changed LDAC very much, occasionally increasing it or decreasing it by one or two. It seems LDAC could have been tuned much more than changing it by one or two. For example Fig. 3 shows a threshold distribution and it appears to have relatively large tails which could have been brought in by changing LDAC. However, when Jesse Harris arrived at the irradiation, he eventually noticed that the LDAC could be changed by a bit more to decrease the standard deviation of our threshold distribution. One other interesting feature of these plots is our standard deviation max is about 25 VCAL units, and the x-ray group starts out lower but increases past this by 40 MRad, and for most of the irradiation, up to 287 MRad, where we stopped, the x-ray group standard deviation was in the 30 to 40 range. This also could have been an issue with their tuning algorithm since their standard deviation does eventually start dropping again.

There are some differences between our irradiation and the X-ray groups' irradiation, but it is hard to say how much of this is truly how much the CROC has deteriorated. It also could be that the fact that they were not irradiating the CROC evenly which would affect the ability to decrease the standard deviation of the thresholds since now some pixels are at different stages of degradation and would react differently to changes in GDAC, LDAC, and TDAC.

Post irradiation

CROCs have been known to break after the irradiation stops. The x-ray groups' CROC stopped working after the irradiation, although this could be due to the ice buildup melting on the card. The gamma-irradiated CROC functioned for a while after the irradiation but eventually broke. The CROC can no longer configure one of the factors, which is the damaged wire bonds on the card. We had hoped the issue was outgassing, and it seems now that it could be a different issue since we did all that we could do to mitigate it.

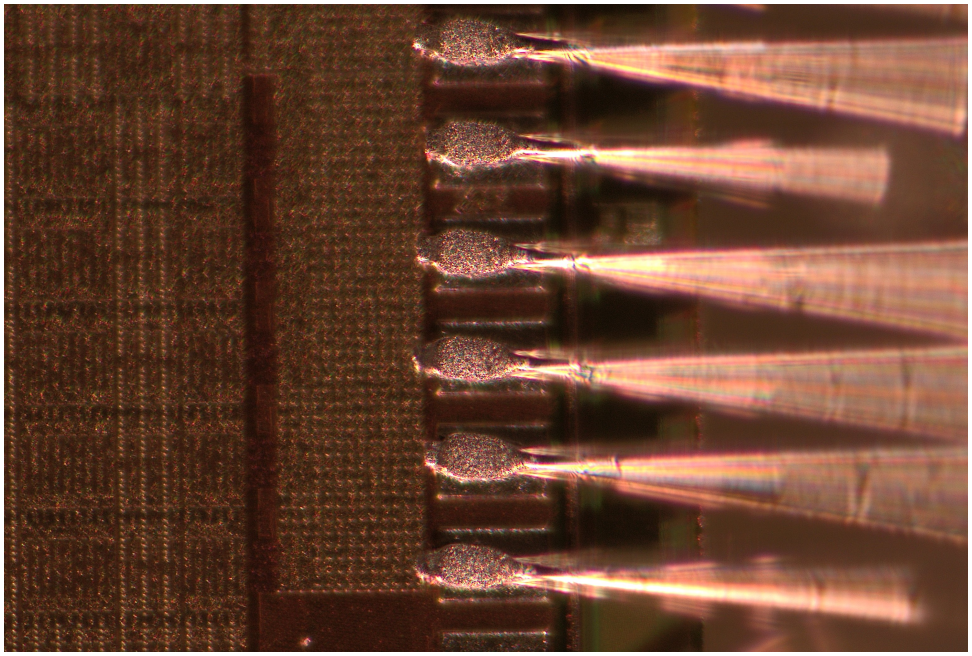

Figure 14: This is an image of the wire bonds connecting to the CROC. You can see very little if any damage to the wirebonds.

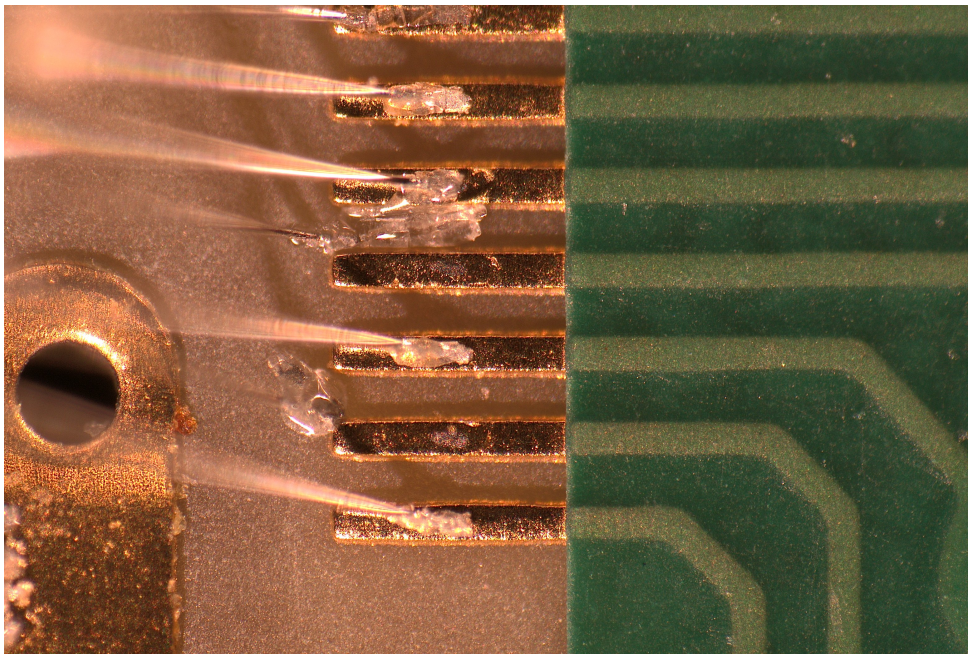

Figure 15: This is an image of the wire bonds on the SCC wire bond pads. You can see a lot more damage, especially compared to 14. Some wire bonds you can see have come up, and there seems to be some substance on the bond pads.

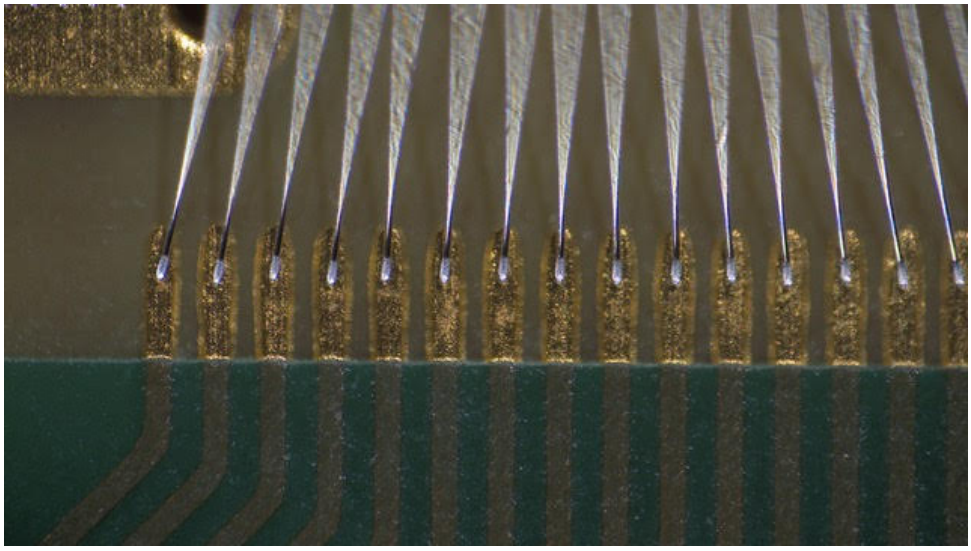

Figure 16: This is an image of the wire bonds on a card wire bonded by another group before irradiation. The wire bonds are in contact with the wire bond pads and have no damage as compared to the post-irradiation photos

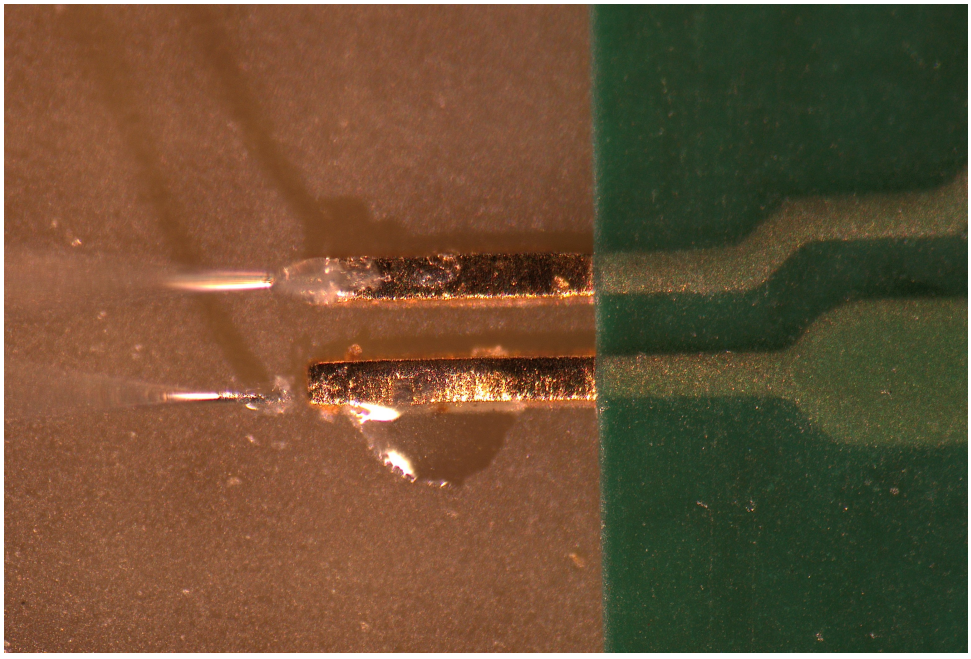

Figure 17: This image shows a large puddle of a clear substance next to some wire bond pads. As you can see there is also damage to the wire bonds with both of them broken off.

After the irradiation, we were able to perform scans and communicate with the CROC for a couple of weeks. However, we eventually stopped being able to run some of

the scans, and eventually, one of the supply voltages dropped to 0. Until this point, we had kept it consistently at -20 Celsius, but we could now run any scans on the CROC. To attempt to fix this, thinking it was a weak connection, we took the CROC out to check the connections. After trying a couple of things to no avail, we took the card to the microscope to look at the wire bonds. The wire bonds had been a problem in the past. We noticed there was some damage to the wire bonds, which we think was the main cause of the breakdown of the CROC. We took it to a microscope with an HD camera to take pictures of the wire bond damage. Fig 14 shows the wire bonds on to the CROC, which is an aluminum-to-aluminum connection, and it seems that these wire bonds are perfectly fine. Fig. 15 shows the wire bonds on the wire bond pad, which seems to be an aluminum wire bond to the ENiG (Electroless nickel immersion gold) pad connection. This connection, compared to the CROC connection (Fig. 14), is drastically different, with wire bonds becoming detached and corroded. This is also noticeable when we compare the post-irradiated wire bonds in Fig. 15 to the image of what they approximately looked like in Fig. 16. This other CROC in Fig. 16 has all of the wire bonds connected to the pads with no noticeable corrosion on the wire bonds or pads and is what the CROC we irradiated looked like before the irradiation.

This damage seems to be some kind of intermetallic reaction or almost galvanic corrosion. The issue could be something called an intermetallic compound between gold and aluminum. This has been known to occur at high temperatures, with the gold combining with the aluminum to make more fragile compounds than the original connection. Although the atoms are not at a high temperature, the irradiation does have an effect since we had this CROC for a month before the irradiation and never saw any signs of damage.

This could be the cause but it is uncertain at this time. One part which does seem inconsistent with this idea is the accumulation of a clear compound on the wire bonds shown in Fig. 17. This is not water and the intermetallic compounds that I was looking at are not clear. We are unsure at this time but it seems to be some radio chemistry between the aluminum and something on the circuit board.

Future Steps

Although our CROC didn't seem to be reacting to the irradiation as much as the x-ray groups, it is unclear why this was. We were not able to achieve a total integrated dose of 1 GRad, but as far as our results showed, we were on track to achieve 1 GRad. We do plan on performing another irradiation this summer with a few alterations. However, the results from this irradiation seem to be promising, with our CROC handling the 287MRad dose and still performing scans during the irradiation.

The CROC we tested was RD53B V1, but the RD53B V2 is coming out with some fixes. This means we could be testing the newest version of this technology. Alongside the new CROC, we plan on performing Parylene coating, which hopefully will eliminate the issues with the wire bonds that come up after the irradiation. Parylene has been tested to be rad-hard and doesn't outgas the electronics. With a parylene-coated RD53B V2 CROC, we also hope to get into an irradiation cell with a higher dose rate. The higher dose rate would allow us to reach 1 GRad and say if these cards can reach 1 GRad of gamma irradiation.

Conclusion

The High Luminosity upgrade for the LHC will increase the luminosity by a factor of 5 to 7, and alongside this, the CMS is going into its phase two upgrade. These upgrades include a new silicon pixel readout chip, the RD53B, which has implemented several improvements from the RD53A. This increased luminosity means the electronics near the beamline will receive a much higher dose rate, which may cause issues. Over the course of a couple of years, these electronics will receive a total integrated dose on the order of 1 Grad. That much radiation can cause a lot of issues with electronics, and something may fail. Testing the electronics to determine how they handle this irradiation is an important part of preparing for these upgrades. Seeing how the electronics change throughout test irradiation allows us to determine how well these electronics might behave after a couple of years in the high luminosity LHC. Although our results are not definitive, our electronics seemed to behave better than a previous x-ray irradiation on average. The reason for this is unclear, but it seems like our electronics could have made it to 1 GRad of total integrated dose. With the next irradiation, we hope to learn more about the effects of gamma radiation on the card up to 1GRad.

References

[1] Daniel Antrim. *Recent RD53B Test Results*. 2020.

[2] Colin England. "Liquid Nitrogen Cooling for Irradiation of Silicon Pixel Detectors for the CMS Experiment". University of Colorado at Boulder, 2023.

[3] Frank Hartmann. *Evolution of Silicon Sensor Technology in Particle Physics, Second Edition*. Springer International Publishing, 2017.

[4] S. Orfanelli. "The Phase 2 upgrade of the CMS Inner Tracker". In: (2020).

[5] Alkis Papadopoulos. *CROC X-Ray Irradiation*. 2022.

[6] CERN RD53. *The RD53B-CMS Pixel Readout Chip Manual*. CERN. 2021.